Creep Resistant Mg-Al-Ca Alloys: Computational Thermodynamics and Experimental Investigation

Koray Ozturk, Yu Zhong, Alan A. Luo, and Zi-Kui Liu

The thermodynamic properties of the ternary Mg-Al-Ca system are investigated in this article, based on the Al-Ca, Al-Mg, and Ca-Mg binary systems. The equilibrium phases in the Mg-Al-Ca alloys studied are the primary magnesium matrix and C15-Al_2Ca, as indicated by the calculated ternary phase diagrams. The experimental results are in good agreement with the thermodynamic calculations using Thermo-Calc *software.*

INTRODUCTION

Magnesium is the eighth most abundant element in the Earth's crust and the third most plentiful element dissolved in seawater.[1] It is the lightest structural metal, with a density of 1.741 g/cm^3, in comparison with the densities of aluminum (2.70 g/cm^3) and iron (7.86 g/cm^3). This makes magnesium alloys particularly attractive for weight reduction and higher fuel efficiency transportation applications.[2–4] The world consumption of magnesium alloys in the automobile industry has experienced a 15% annual increase over the last decade.[5] Thus, there is an urgent need for efficient alloy development. The emerging concept of system materials design provides such opportunities.[6] In the system materials design, the essential component is the computational thermodynamics, often referred to as Calculation of Phase Diagrams, or CALPHAD.

Recently, research has been conducted on Mg-Al-Ca-based alloys with or without additional alloying elements.[7–14] The addition of calcium to Mg-Al-based alloys improved the high-temperature properties, such as creep resistance.[15] However, few studies have been done on the thermodynamics and phase relationships in this alloy system.[15–18] In the described work, the phase equilibria of two Mg-Al-Ca alloys were compared with the thermodynamic calculations based on the CALPHAD approach[19] and the *Thermo-Calc* software.[20]

CALCULATED PHASE DIAGRAMS

Figure 1 shows the calculated phase diagrams of the three binary systems. The thermodynamic description of the Mg-Al-Ca ternary system was obtained by combining the data of the three binary systems assuming no ternary solubility in the all binary compounds due to the lack of experimental data. No ternary interactions were introduced either.

Figures 2–6 show five isothermal sections of the magnesium-rich corner of the ternary Mg-Al-Ca phase diagram at room temperature (298 K), 563 K, 643 K, 673 K, and 773 K, based on the thermodynamic calculations using *ThermoCalc* software. The 298 K section (Figure 2) suggests that both GM-B and GM-C alloys fall into the three-phase region (α-Mg + C15-Al_2Ca + γ-AlMg) for equilibrium microstructure at room temperature. As the temperature increases, the (α-Mg + C15-Al_2Ca) region widens significantly (Figures 3 and 4), and the face-centered cubic (fcc) C15-Al_2Ca is supposed to be the stable phase at both 563 K and 643 K. However, note that the GM-C alloy is located near the border of the region where the hexagonal C14-Mg_2Ca becomes an equilibrium phase.

The calculated isothermals (Figures 3, 4, and 6) were also compared to the

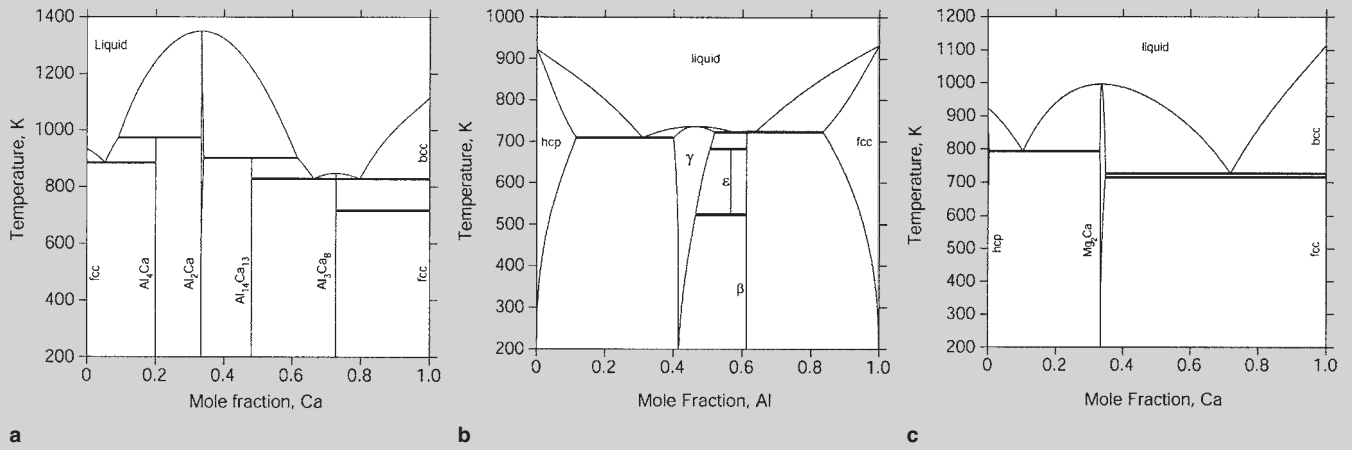

Figure 1. The calculated phase diagrams of the (a) Al-Ca, (b) Al-Mg, and (c) Ca-Mg binary systems.

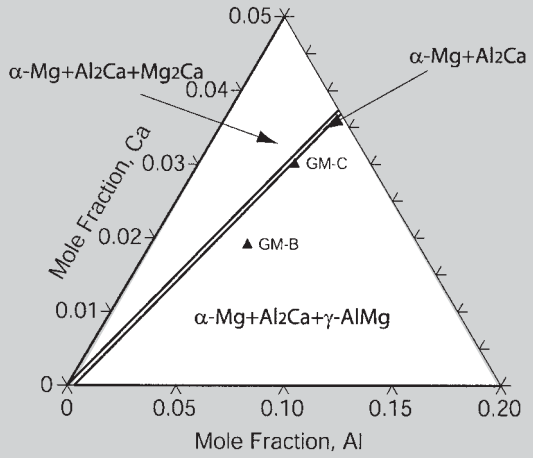

Figure 2. A calculated isothermal section at 298 K showing the alloy composition.

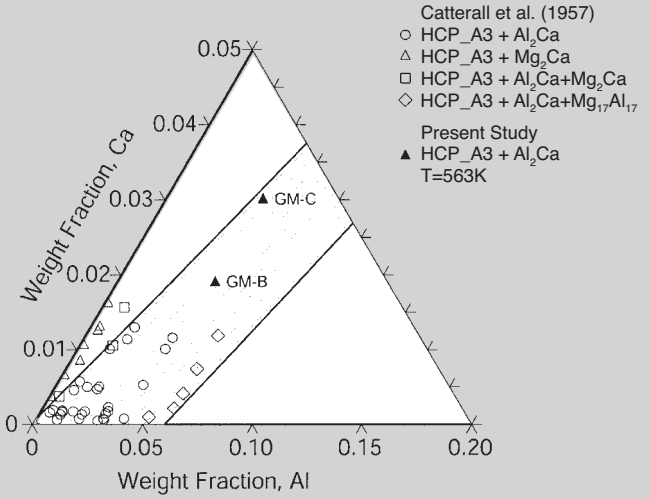

Figure 3. A calculated isothermal section at 563 K and the experimental data by Catterall et al.[16] and by this study.

experimental results of Catterall et al.[16] on Mg-Al-Ca alloys. The agreement is good except for the extent of the α-Mg phase field at 643 K (Figure 4). The calculation predicted less calcium in the α-Mg phase than the measured values. This inconsistency may be due to experimental errors such as calcium loss during the alloy preparation.[16] A comparison with the investigation of Ninomiya et al.[17] is shown in Figure 5. The calculated phase boundary between the two-phase (hcp + C15-Al_2Ca) and three-phase (hcp + C15-Al_2Ca + C14-Mg_2Ca) regions is in agreement with the experimental data points by Ninomiya et al.[17]

The predicted liquidus projection of the Mg-Al-Ca system is presented in Figure 7 with respect to the composition triangle. The liquidus surface is divided into 11 primary crystallization fields: Ca(fcc), Ca(bcc), Mg(hcp), Al(fcc), C15-Al_2Ca, C14-Mg_2Ca, Al_3Ca_8, $Al_{14}Ca_{13}$, Al_4Ca, AlMg-γ, and AlMg-β. The liquidus surface is dominated by the C15-Al_2Ca phase extensively and by the C14-Mg_2Ca phase to some extent. These are the highest melting point compounds with relatively high stabilities in this ternary system.

AS-CAST MICROSTRUCTURE

Both GM-B and GM-C have similar microstructures; Figure 8 shows optical micrographs of GM-C alloy samples under different conditions. The primary α-Mg grains are surrounded by the interconnected network of the grain boundary phase in the as-cast condition. This phase, which forms during the eutectic solidification process, has a lamella-type morphology (Figure 8a).

Figure 9 is the x-ray diffraction (XRD) pattern for the as-cast GM-C alloy. No distinct peaks of the fcc C15-Al_2Ca phase were detected. Instead, the XRD analysis showed some unknown peaks, of which two approximately matched the hexagonal C14-Mg_2Ca phase. A similar XRD pattern was also obtained for the GM-B alloy. Replicas of the as-cast GM-C sample were prepared by overetching, which dissolves the matrix phase and the eutectic magnesium but leaves the intermetallic phase on the adhesive carbon tapes. Figure 10 shows both the scanning-electron microscopy (SEM) image of the hollow lamellae and the energy-dispersive spectroscopy (EDS) microanalysis results at different spots. The EDS spectrum shows distinctive peaks from magnesium, aluminum, and calcium, indicating the possible formation of a ternary Mg-Al-Ca phase since the matrix effect is eliminated from the analysis.

A detailed XRD and transmission

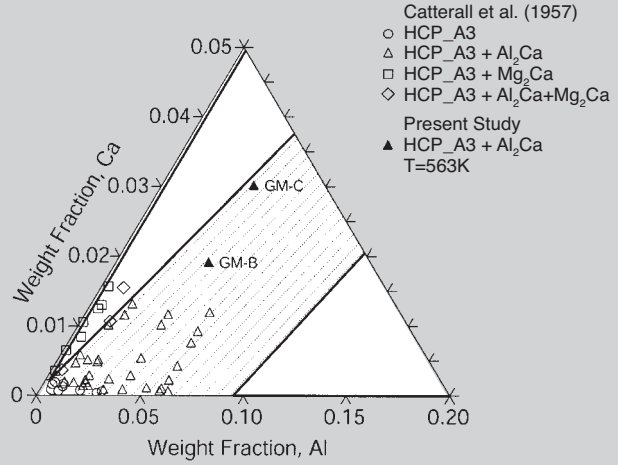

Figure 4. A calculated isothermal section at 643 K and the experimental data by Catterall et al.[16] and by this study.

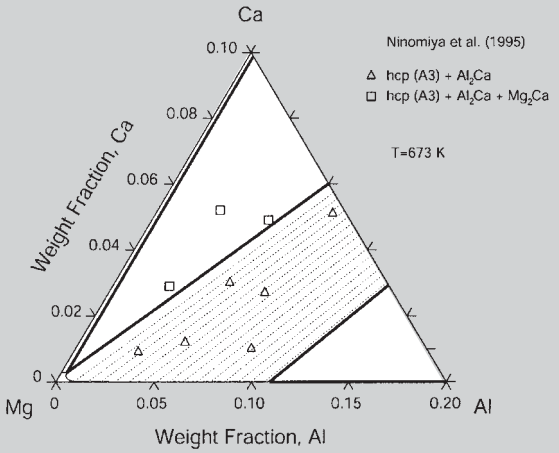

Figure 5. A calculated isothermal section at 673 K showing the experimental data by Ninomiya et al.[17]

EXPERIMENTAL PROCEDURES

Calculation of Phase Diagrams, which has been under development since the early 1970s,[21] was used to develop a thermodynamic description of the Mg-Al-Ca system.

The thermodynamic descriptions of the pure magnesium, aluminum, and calcium elements are taken from the SGTE database.[22] In the Mg-Al-Ca ternary systems, there are three binary systems: Al-Ca, Al-Mg, and Ca-Mg. The thermodynamic descriptions of Al-Mg[23,24] are available in the literature, Ca-Mg is modified from the work of Agarwal et al,[25] and the Al-Ca system was studied in the present work.

Two alloys, Mg-4.5Al-1.9Ca (GM-B) and Mg-4.5Al-3.0Ca (GM-C) (all in weight percent unless otherwise specified), were made by die casting at Lexington Die Casting, Lakewood, NY. The melt temperature was controlled at around 950 K with the die surface temperature maintained at 623 K. The chemical analysis using inductively coupled plasma/atomic emission spectroscopy techniques was performed with the following results. For the GM-B alloy, the chemical composition was (in weight percent) Mg-4.5Al-1.9Ca-0.27Mn-0.003Fe-<0.002Ni-0.002Cu. For GM-C the composition was Mg-4.5Al-3.0Ca-0.27Mn-0.003Fe-<0.002Ni-0.003Cu.

Three types of samples were prepared for each alloy: as-cast, heat treated at 560 K, and heat treated at 643 K. The alloys were sealed under an inert atmosphere during the heat treatment for one week. At the end of the heat treatments, the samples were quenched into water to retain the equilibrium structure. Microstructural observations were made using optical (Olympus BX60M) and scanning electron microscopes (Hitachi S-3500N and Philips XL20). Each sample was first cut from the as-cast and the quenched alloys using a regular lab-scale diamond saw. The samples were then polished and etched using 4 vol.% Nital solution (HNO3 in ethanol). For optical microscopy purposes, etching was performed only by applying the etchant on the surface for a short period of time (~10 s). This is because of the severe selective etching nature of these alloys. Primary magnesium grains dissolve very quickly on contact with the etchant as compared to the secondary phase.

The selective etching nature of the samples was utilized during the phase identifications by x-ray diffraction (Scintag PadV) and qualitative chemical analysis by energy-dispersive spectroscopy (EDS). The prolonged etching (~20 s) was performed by dipping the samples in the etchant to increase the surface area of the intermetallic precipitates and its intensity on the x-ray spectrum. Chemical mapping and spot analysis were also performed using EDS. Both the bulk sample surfaces and their replicas were checked and compared with each other. Replicas were prepared from the etched samples by placing an adhesive carbon tape on their surface and detaching the tape from the samples.

electron microscopy (TEM) investigation by Luo et al. on this lamellae-type grain boundary phase[15] suggested that the intermetallic phase was a ternary solid solution phase in the hexagonal C14-Mg_2Ca structure. It was represented by the chemical formula of $(Mg, Al)_2Ca$, where some of the magnesium atoms are replaced by aluminum atoms in the crystal lattice. This is in agreement with the present EDS study although the crystal structure of the $(Mg, Al)_2Ca$ phase is not verified in this study.

The experimental results do not agree with the calculated equilibrium phase diagram in Figure 2. Instead of the fcc C15-Al_2Ca and γ-AlMg equilibrium phases as suggested by the phase diagram, a hexagonal ternary $(Mg, Al)_2Ca$ lamellae structure is formed in the die-casting microstructure of the GM-C alloy. It is not unusual that the fast cooling rates of die casting (on the order of 100 K/s) can produce microstructures different from those expected in the equilibrium solidification conditions.[26] Also, the GM-C alloy is closely located near the borderline of the three-phase region where the hexagonal C14-Mg_2Ca is an equilibrium phase.

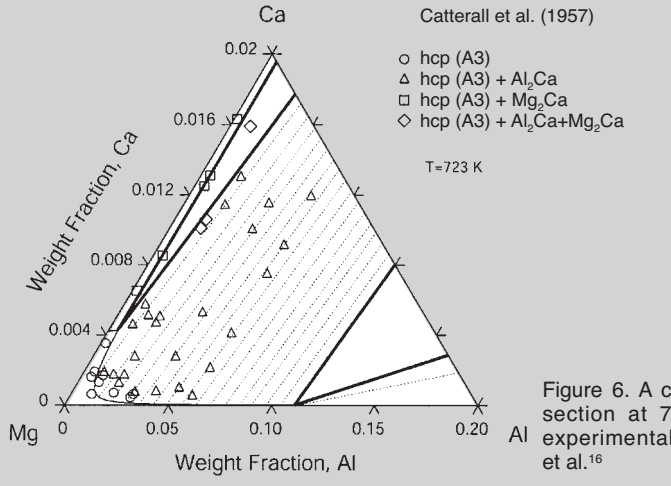

Figure 6. A calculated isothermal section at 723 K showing the experimental data by Catterall et al.[16]

MICROSTRUCTURE OF HEAT-TREATED SAMPLES

Figure 8 shows the network morphology of the ternary grain boundary phase in the as-cast microstructure (Figure 8a) during heat treatment. After exposure at 563 K for one week, the network is less complete and the lamellas decompose and become spherical (Figure 8b). This effect is more pronounced when the temperature is increased to 643 K (Figure 8c). A similar phenomenon was also observed by Liu et al.[18]

The XRD results for both GM-B and GM-C alloys confirmed the formation of the fcc C15-Al_2Ca phase after the one-week heat treatments at 563 K and 643 K, in agreement with the calculated phase diagram shown in Figures 3 and 4. Figure 11 shows the EDS microanalysis results of the small particles in the bulk alloys samples, where the magnesium peak is from the surrounding matrix because of electron beam spreading. In the replica sample where the matrix interference is eliminated, the precipitates in the heat-treated samples contained only aluminum and calcium (Figure 12). In addition, a quantitative analysis of the particles was performed on the replica, showing the aluminum-to-calcium ratio at about 2:1. This result is a strong support of the XRD analysis for the existence of the fcc C15-Al_2Ca phase in the heat-treated samples.

IMPLICATIONS ON CREEP RESISTANCE

The fact that the Mg-Al-Ca ternary phase in the as-cast microstructure decomposes into fcc C15-Al_2Ca after long-term exposures at 563 K or 643 K does not necessarily suggest instability of this ternary phase in the operating temperatures of automotive powertrains (< 523 K). In fact, the metallurgical stability of the ternary $(Mg, Al)_2Ca$ phase and its interfacial coherency with the magnesium matrix were reported to be responsible for the improved

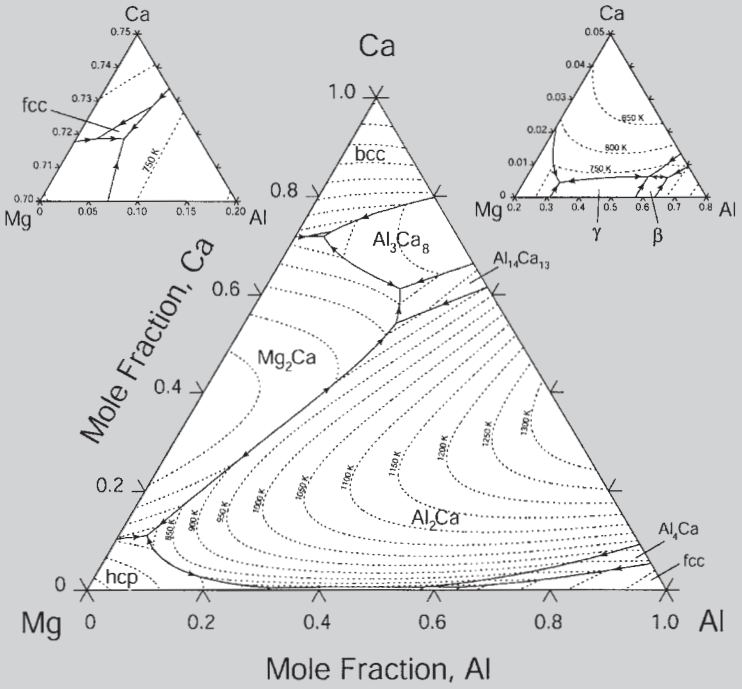

Figure 7. The liquidus projection of the Mg-Al-Ca ternary system with isotherms (dotted lines).

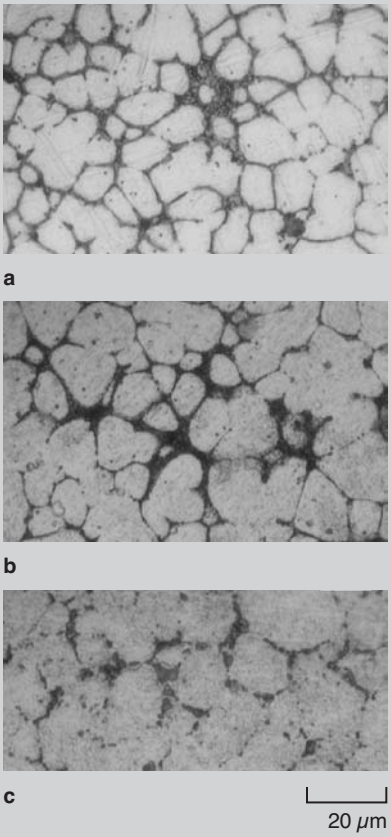

Figure 8. Optical micrographs of the GM-C alloy samples (a) as-cast, (b) heat treated at 563 K for one week, and (c) heat treated at 643 K for one week.

creep resistance of Mg-Al-Ca alloys at temperatures up to 473 K.[15] On the other hand, Mg-Al-Ca alloys containing fcc C15-Al_2Ca in the die-cast microstructure also demonstrated good creep resistance and tensile strength up to 423 K,[11] indicating that the fcc C15-Al_2Ca can provide significant strengthening in the grain boundaries. The thermal stability of both (Mg, $Al)_2Ca$ and fcc C15-Al_2Ca intermetallic phases can be inferred from their high melting points and the eutectic temperatures. Mg_2Ca has a eutectic temperature of 718 K and a melting temperature of 988 K, while Al_2Ca has a eutectic temperature of 973 K and a melting temperature of 1,352 K.[14,27] Thermally stable phases present at the grain boundary provide effective pinning to resist grain boundary sliding, hence, the improved creep resistance. However, further research is needed on the transformation kinetics of (Mg, $Al)_2Ca$ to fcc C15-Al_2Ca at the operating temperatures of automotive powertrains and their effects on creep.

The liquidus projection of the Mg-Al-Ca ternary system (Figure 7) is presented as a starting point for future experimental verification and refinement. It is noteworthy from the calculations that the addition of calcium to liquid Mg-Al alloys in very small amounts (e.g., 1 mol.%) causes formation of the fcc C15-Al_2Ca phase during solidification. Because the formation of the γ phase is detrimental to the creep strength at elevated temperatures, it is important to completely remove the γ phase from the magnesium-based Mg-Al-Ca alloys for high-temperature applications. It is calculated from the "L = hcp + Al_2Ca" reaction that the phase formation is avoided if the ratio of Al/Ca is less than ~2.1.

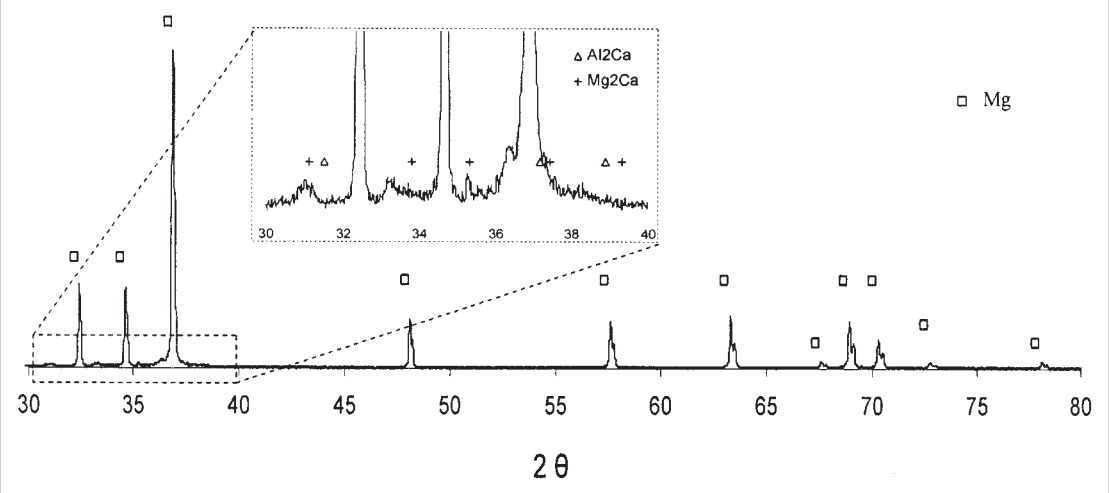

Figure 9. An X-ray diffraction pattern of the as-cast GM-C alloy showing the (Mg, $Al)_2Ca$ phase based on the hexagonal C14-Mg_2Ca structure.

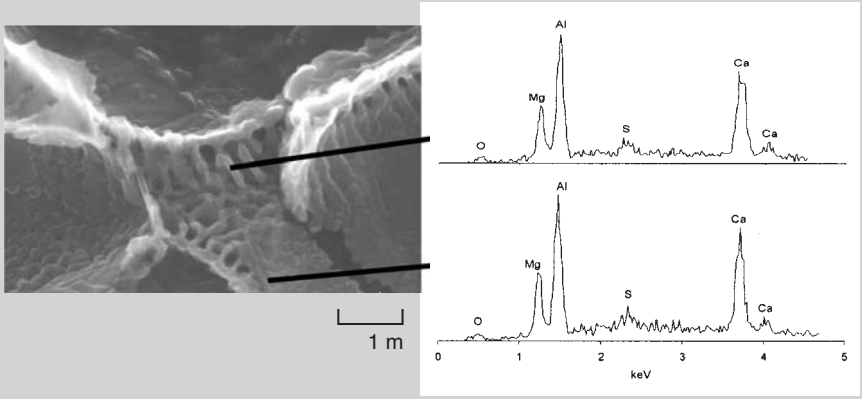

Figure 10. An SEM image and EDS microanalysis of the lamellae-type grain boundary phase from a carbon tape replica of an as-cast GM-C sample, showing the formation of the Mg-Al-Ca ternary phase.

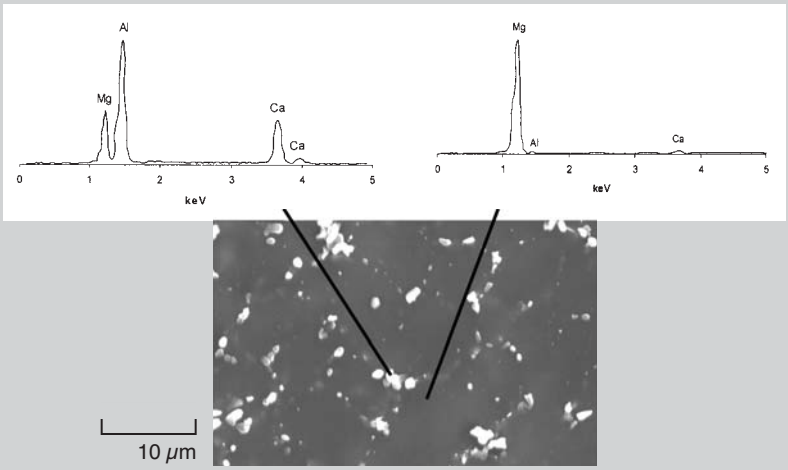

Figure 11. An SEM image and EDS microanalysis of the particulate grain boundary phase in a bulk GM-B sample after heat treatment at 643 K for a week. The magnesium peak is from the surrounding matrix.

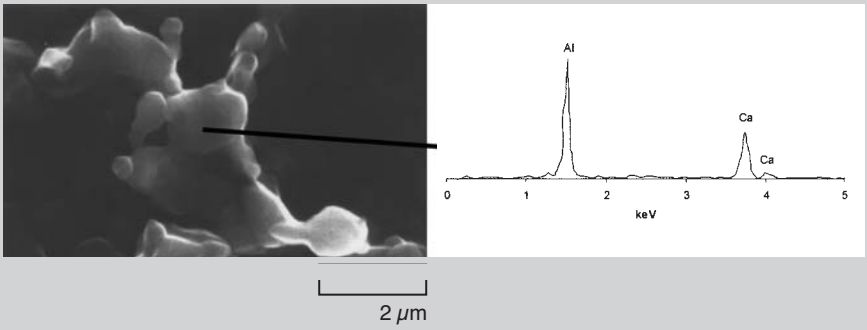

Figure 12. An SEM image and EDS microanalysis of the particulate grain boundary phase from a carbon tape replica of a GM-B sample after heat treatment at 643 K for a week, showing the formation of fcc C15-Al_2Ca phase.

ACKNOWLEDGEMENTS

This work is supported by the U.S. National Science Foundation CAREER Award under the grant DMR-9983532. The software program used for all calculations is licensed from the Foundation for Computational Thermodynamics, Stockholm, Sweden. The authors also acknowledge Anil Sachdev and Bob Powell for reviewing the manuscript and General Motors Corporation for permission to publish this paper.

References

1. D. Kramer, *U.S. Geological Survey—Minerals Information* (Washington, D.C.: USGS, 1997).
2. G. Craig, *Use of WE-43A-T6 Magnesium in the MD600 Helicopter Drive System* (Coronado, CA: International Magnesium Association, 1998), pp. 19–23.
3. H. Friedrich and S. Schumann, *The Use of Magnesium in Cars—Today and in the Future* (Coronado, CA: International Magnesium Association, 1998), pp. 1–7.
4. A. Luo, *Magnesium Technology 2000,* ed. H.I. Kaplan, J. Hryn, and B. Clow (Warrendale, PA: TMS, 2000), pp. 89–98.
5. P. Aroule, *IMA-55, A Global Vision for Magnesium* (Washington, D.C.: International Magnesium Association, 1998), pp. 36–46.
6. G.B. Olson, *Science,* 277 (1997), pp. 1237–1242.
7. F.M. Knoop et al., *Powder Metallurgy World Congress (PM '94)* (Paris: Editions de Physique (France), 1994), pp. 2237–2240.
8. T. Ebert, K.U. Kainer, and B.L. Mordike, *Magnesium Alloys and their Applications* (Frankfurt, Germany: Werkstoff-Informationsgesellschaft mbH, 1998), pp. 563–568.
9. C. Shaw and H. Jones, *Materials Science and Technology,* 15 (1999), pp. 78–84.
10. T. Tsukeda et al., *Magnesium Technology 2000,* ed. H.I. Kaplan, J.N. Hryn, and B.B. Clow (Warrendale, PA: TMS, 2000), pp. 395–402.
11. M.O. Pekguleryuz and J. Renaud, *Magnesium Technology 2000,* ed. H.I. Kaplan, J.N. Hryn, and B.B. Clow (Warrendale, PA: TMS, 2000), pp. 279–284.
12. A. Luo and T. Shinoda, *Magnesium Alloy Having Superior Elevated-Temperature Properties and Die Castability,* U.S. patent 5,855,697 (Imra America, Inc., United States, 1999).
13. A. Luo, M.P. Balogh, and B.R. Powell, *SAE2001* (Detroit, MI: SAE, 2001).
14. B.R. Powell et al., *SAE2001* (Detroit, MI: SAE, 2001).
15. A.A. Luo, M.P. Balogh, and B.R. Powell, *Metall. Mater. Trans. A,* 33 (2002), pp. 567–574.
16. J.A. Catterall and R.J. Pleasance, *J. Inst. Metals,* 86 (1957-58), pp. 189–192.
17. R. Ninomiya, T. Ojiro, and K. Kubota, *Acta Metall. Mater.,* 43 (1995), pp. 669–674.
18. M. Liu, et al., *J. Mater. Sci. Lett.,* 21 (2002), pp. 1281–1283.
19. N. Saunders and A.P. Miodownik, *CALPHAD (Calculation of Phase Diagrams): A Comprehensive Guide* (Oxford and New York: Pergamon, 1998).
20. J.O. Andersson et al., *Calphad-Computer Coupling of Phase Diagrams and Thermochemistry,* 26 (2002), pp. 273–312.
21. L. Kaufman and H. Bernstein, *Computer Calculation of Phase Diagrams with Special Reference to Refractory Metals* (New York: Academic Press, 1970).
22. A.T. Dinsdale, *Calphad-Comput. Coupling Ph. Diagrams Thermochem.,* 15 (1991), pp. 317–425.
23. P. Liang et al., *Z. Metallkd.,* 89 (1998), pp. 536–540.
24. I. Ansara, A.T. Dinsdale, and M.H. Rand, editors, *COST 507: Thermochemical Database for Light Metal Alloys,* Vol. 2 (Brussels, Belgium: European Commission, 1998).
25. R. Agarwal et al., *Z. Metallkd.,* 86 (1995), pp. 103–108.
26. A. Luo, *Proc. of the Third International Magnesium Conference* (London: The Institute of Materials, 1997), pp. 449–464.
27. T.B. Massalski et al., *Binary Alloy Phase Diagrams. Vol. I* (Metals Park, OH: American Society for Metals, 1986).

Koray Ozturk, Yu Zhong, and Zi-Kui Liu are with the Department of Materials Science and Engineering at Pennsylvania State University. Alan A. Luo is a staff research engineer at General Motors Research and Development Center.

For more information, contact A.A. Luo, General Motors Research and Development Center, Materials and Processes Lab, 30500 Mound Road, Warren, Michigan 48090-9055; (586) 986-8303; fax (586) 986-9204; e-mail alan.luo@gm.com